Journal of Hazardous Materials 184 (2010) 386–391

Contents lists available at ScienceDirect

Journal of Hazardous Materials

journal homepage: www.elsevier.com/locate/jhazmat

Degradation of malachite green on Pd/WO_3 photocatalysts under simulated solar light

Yonggang Liu[a,b], Yoshihisa Ohko[b,*], Ruiqin Zhang[c], Yingnan Yang[a], Zhenya Zhang[a,**]

[a] Graduate School of Life and Environmental Science, University of Tsukuba, 1-1-1 Tennodai, Tsukuba, Ibaraki 305-8572, Japan
[b] Research Institute for Environmental Management Technology, National Institute of Advanced Industrial Science and Technology (AIST), 16-1 Onogawa, Tsukuba, Ibaraki 305-8569, Japan
[c] Department of Chemistry, Zhengzhou University, Zhengzhou, Henan 450001, China

ARTICLE INFO

Article history:
Received 12 April 2010
Received in revised form 14 June 2010
Accepted 14 August 2010
Available online 21 August 2010

Keywords:
Photocatalysis
Visible light
Malachite green oxalate
Tungsten trioxide
Dye sensitization

ABSTRACT

The photocatalytic degradation of malachite green (MG) dye molecules in aqueous solution was investigated by using palladium (Pd) modified tungsten trioxide (WO_3) under simulated solar light. The optimum values for Pd content vs. WO_3 and catalyst concentration in solution for MG (5.0 μmol L^{-1}) degradation were 0.5 wt.% and 150 mg L^{-1}, respectively. The MG concentration change followed the pseudo first order kinetics of the Langmuir-Hinshelwood model. Since MG was also degraded under visible light (λ > 470 nm), which was not absorbed by WO_3, the mechanism involved both the photocatalytic degradation and self-sensitized degradation of MG. Pd modified WO_3 would be useful as an efficient tool for the decolorization of wastewater under solar light.

1. Introduction

The photocatalytic decomposition of various organic compounds in industrial wastewater has been extensively studied, since the pollutants can be oxidized quickly and non-selectively [1–8]. Among various semiconductors, titanium oxide (TiO_2) has been employed as a typical photocatalyst for both fundamental research and practical applications owing to its excellent stability and high photoactivity under ultraviolet (UV) light. However, its widespread use is limited due to its large bandgap (3.2 eV), which means that it absorbs only UV light [9]. Therefore, there has been a strong demand for new classes of semiconductor materials, and especially those responding to visible light. Considerable effort has been expended to fabricate such photocatalysts, mainly based on TiO_2, by anionic or cationic impurity doping [10–12], or in combination with smaller-bandgap semiconductors [13]. However, in spite of extensive research, most systems have insufficient practical efficiency.

Tungsten trioxide (WO_3) has been studied as one of the best candidates for visible light-driven photocatalysis. It has an indirect band gap with a relatively small energy (2.4–2.8 eV) [14], and many advantages including a deeper valence band (+3.1 eV), strong adsorption within the solar spectrum, stable physicochemical properties, and resilience to photocorrosion effects [9]. However, pure WO_3 was once considered to be inactive as regards the oxidation of organic contaminants, because the conduction band level of WO_3 (+0.5 V vs. NHE) is more positive than the potential for the single-electron reduction of oxygen (O_2/O_2^- = −0.284 V vs. NHE; O_2/HO_2 = −0.046 V vs. NHE) [15,16]. In contrast, several groups have recently reported that suitable cocatalysts [16–20] can enhance the photocatalytic activity of WO_3 for small alcohol species by the multiple electron reduction of oxygen (O_2/H_2O_2 = +0.68 V vs. NHE; O_2/H_2O = +1.23 V vs. NHE) [16]. It is very important to investigate the possibility of employing the WO_3-based photocatalyst to degrade other harmful organic species or bacteria.

The triphenylmethane dye, malachite green (MG), which is a carcinogenic organic molecule, is still used illegally for various purposes including in aquaculture as a fungicide on larvae and juvenile fish, as a parasiticide, and in the food, textile and other industries [4,21]. Therefore, there are both environmental and health concerns in relation to this particular dye. In general, dye molecules that become excited by adsorbing visible light are capable of injecting their electrons into the conduction band of a semiconductor when the excited state of dye is sufficiently negative compared with the conduction band of the semiconductor. This process is known as dye sensitization. The mechanism has been used as a feasible approach for increasing the photocatalytic reaction efficiency of dye degradation. With TiO_2, self-sensitized dye bleaching has

* Corresponding author. Tel.: +81 29 861 8748; fax: +81 29 861 8167.
** Corresponding author. Tel.: +81 29 853 4712; fax: +81 29 853 4712.
E-mail addresses: y-ohko@aist.go.jp (Y. Ohko), tyou6688@sakura.cc.tsukuba.ac.jp (Z. Zhang).

0304-3894/$ – see front matter © 2010 Elsevier B.V. All rights reserved.
doi:10.1016/j.jhazmat.2010.08.047

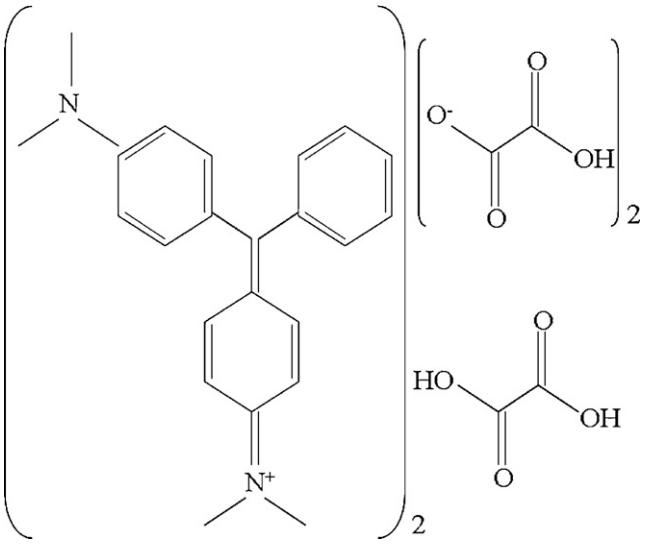

Scheme 1. Structural formula of malachite green oxalate.

been successfully demonstrated to extend the absorption of TiO_2 to the visible region [22]. The photoinduced electrons further form $^{\bullet}O_2^-$ and $^{\bullet}OH$ with O_2 adsorbed on the surface of TiO_2, leading to the oxidation of organic molecules. Considering the very positive conduction band level, WO_3 may be a good candidate for dye sensitization. If Pd is also effective for the dye-sensitized degradation of dye, it will provide a novel strategy for improving visible light absorption and photoinduced degradation using WO_3.

In the present study, the photocatalytic degradation of MG was investigated using Pd modified WO_3 under simulated solar light irradiation. The Pd content and catalyst loading parameters were optimized. Furthermore, a kinetic analysis was carried out, and the self-sensitization effect of dye on the photocatalytic activity of Pd/WO_3 was evaluated for a discussion of the reaction mechanisms.

2. Experimental

2.1. Materials and preparation of photocatalysts

WO_3 powder (Wako Pure Chemical Industries) was used as a photocatalyst. Pd powder was supplied by Sigma–Aldrich (surface area, 40–60 $m^2\,g^{-1}$). A powder of WO_3 modified with Pd (hereafter Pd/WO_3) was prepared by the mechanical mixing of Pd (wt.% vs. WO_3) and WO_3 in a ceramic mortar. MG oxalate was obtained from Wako Pure Chemical Industries and used without any further purification. The structural formula of MG is presented in Scheme 1. Stock solution containing 1.0 mmol L^{-1} of MG in distilled water was prepared, protected from light, and stored at 277 K.

2.2. Characterization of the photocatalysts

UV–visible spectrum of the sample was recorded on a spectrophotometer (UV-2550, Shimadzu Co. Ltd., Japan). X-ray powder diffraction (XRD) measurement was carried out by using an X-ray diffractometer (Rigaku Smartlab). TEM images were obtained from a transmission electron microscope (JEM-1010, JEOL Ltd.). The BET surface area of the sample was determined with a BET area analyzer (Autosorb-1, Quanta Chrome).

2.3. Experimental apparatus and procedure

In the photocatalytic system, a 50 mL beaker was used as the reactor and was equipped with a magnetic stirrer. A simulated solar lamp (XC-100B, SERIC Ltd., Japan) was used as the irradiation source, and the light intensity was measured with a photometer (LI-250A, LI-COR Inc., USA). The photoemission spectrum was measured with an optical fiber spectrometer (Model USB4000, Ocean Optics Inc., USA) (Fig. 1).

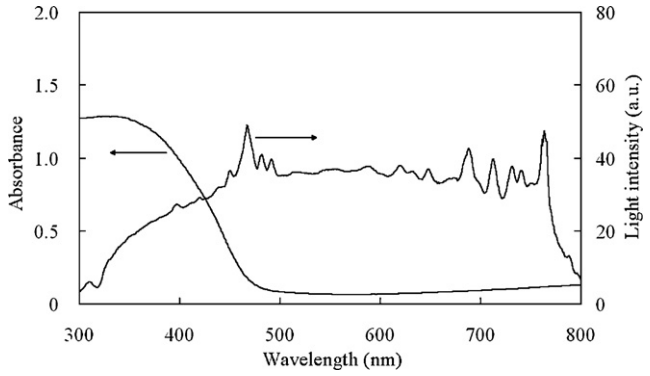

Fig. 1. Absorption spectrum of WO_3 (left vertical axis) and the photoemission spectrum of the irradiation light source (right vertical axis).

The photocatalytic degradation experiments were carried out by adding the stock solution of MG (1.0 mmol L^{-1}) and catalyst in water at the desired concentration (dye concentration = 5.0 μmol L^{-1}, catalyst concentration = 150 mg L^{-1}; otherwise stated). The total volume of the solution for the reaction was adjusted to 30 mL. Before irradiation, the suspension (30 mL) was magnetically stirred for 60 min in the dark to achieve equilibration. Then the lamp was switched on to initiate the reaction. During irradiation, samples were taken and centrifuged at a constant time interval. The dye concentration was measured with a UV–vis spectrophotometer (SmartSpec 3000, Bio-Rad Laboratories Inc., USA) at 618 nm. The absorbance of MG at different irradiation times was recorded on a spectrophotometer (UV-2550, Shimadzu Co. Ltd., Japan) in the 300–800 nm wavelength range.

3. Results and discussion

3.1. Characterization

Fig. 2 shows the XRD patterns of WO_3 and Pd/WO_3 samples. When the XRD patterns of the samples were compared to tungsten oxide JCPD files (No. 43-1035) and those reported by others [23,24], the diffraction patterns of the samples assigned those of WO_3 monoclinic structure. No significant differences were observed in the XRD peaks between the WO_3 and Pd/WO_3 samples, indicating that the Pd doping did not influence the crystal structures of WO_3. In

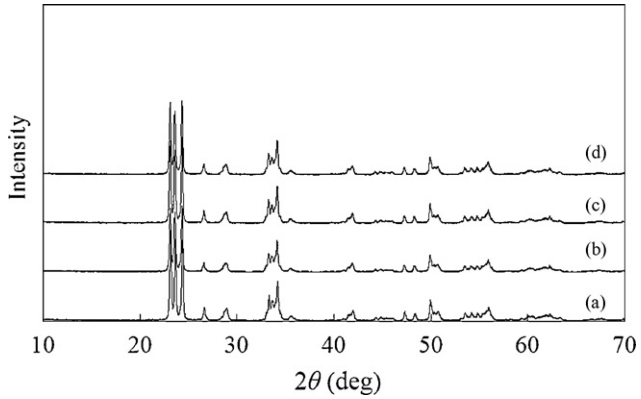

Fig. 2. XRD patterns of WO_3 with different Pd loadings: (a) 0 wt.%, (b) 0.1 wt.%, (c) 0.5 wt.%, (d) 1.0 wt.%.

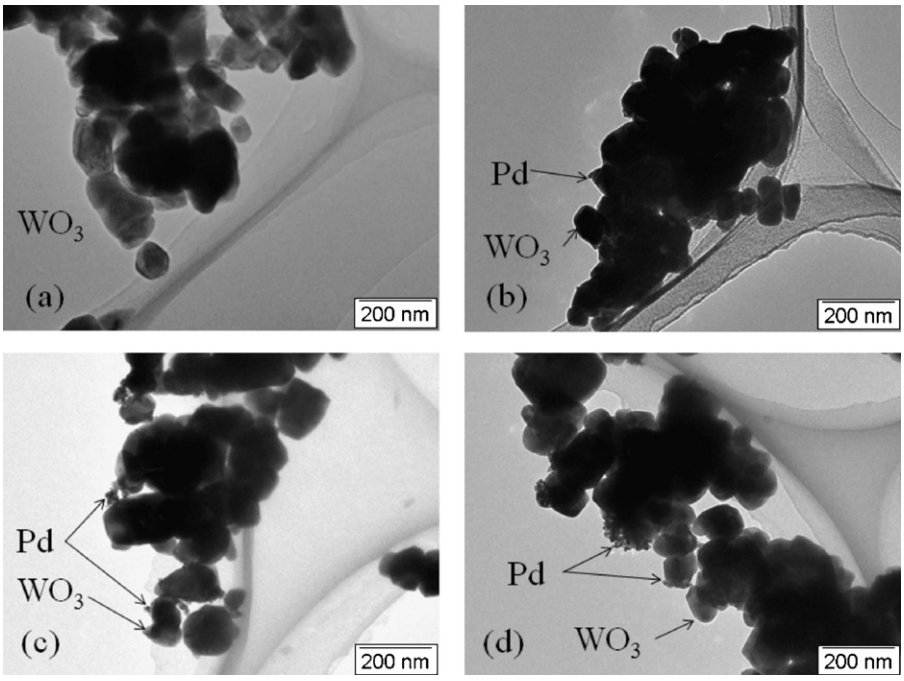

Fig. 3. TEM images of WO_3 with different Pd loadings: (a) 0 wt.%, (b) 0.1 wt.%, (c) 0.5 wt.%, (d) 1.0 wt.%.

addition, no Pd peaks were observed for the Pd/WO_3 samples due to a low content and nano-size of Pd [25,26].

The morphology and microstructure of the as-prepared samples were revealed by TEM. Fig. 3 shows that the WO_3 particles range from 50 to 150 nm and the Pd particles about 10 nm in size. In the Pd/WO_3 samples, most Pd nanoparticles were found to be well-dispersed on the surface of WO_3. However, a little aggregation of Pd nanoparticles was found in places especially for the 1.0 wt.% Pd/WO_3 sample. This is in agreement with the results of Wang et al. [27]. The specific surface area of the WO_3 was about 5 $m^2\ g^{-1}$ which is in agreement with other report [17] and those of the Pd/WO_3 samples slightly increased to 6–7 $m^2\ g^{-1}$ due to the Pd loading and a grind of WO_3 powders in the preparation process.

3.2. Dependence on Pd content

To clarify the effect of Pd content on the photocatalytic activity of Pd/WO_3 photocatalyst, a set of parallel experiments were conducted on the basis of the photodegradation of MG in an aqueous solution. MG photodegradation using pure WO_3 and the WO_3 doped with 0.1, 0.5 and 1.0 wt.% Pd are illustrated in Fig. 4.

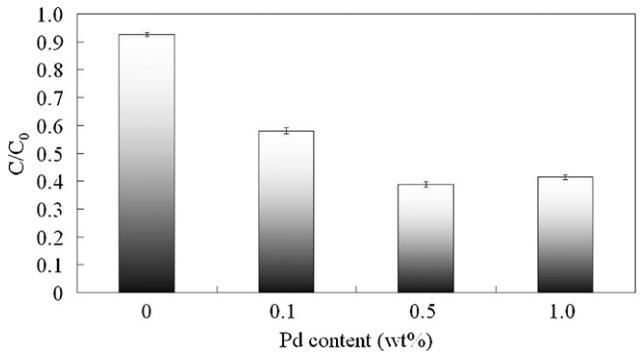

Fig. 4. Dependence on Pd content for the MG degradation after 150 min irradiation. Experimental conditions: dye concentration 5.0 μmol L^{-1}, catalyst concentration 150 mg L^{-1} and simulated solar light intensity 0.4 mW cm^{-2}.

As shown in Fig. 4, the concentration of the MG solution decreases in the presence of pure WO_3 catalyst under solar irradiation, but the degradation efficiency is very low. Only 7% of the MG was degraded after 150 min irradiation. After Pd doping, the composite photocatalysts exhibited significantly enhanced activity. In our result, the performance of the 0.5 wt.% Pd/WO_3 composite sample was particularly noteworthy. Zhao and Miyauchi [9] similarly demonstrated that 0.5 wt.% Pt-loading produces the better photocatalytic activity for both WO_3 nanotubes and commercial nanoparticles than that of 0.1 and 1.0 wt.%. This result constitutes an improvement when compared with the pure WO_3 sample. The superior photoactivity of composite samples compared with the MG degradation efficiency of pure WO_3 is very encouraging and is explained in the following discussion.

In the Pd/WO_3 composite, electron transfer occurs from the conduction band of the light-activated WO_3 to the Pd, which acts as an electron trapping center that can accelerate the charge separation [28]. This efficient charge separation greatly increased the photocatalytic activity of Pd/WO_3 composites. Furthermore, the experimental data demonstrate that the photocatalytic activity is related to the Pd content. When the Pd content is low, the effect of photogenerated electrons trapped by the Pd is not obvious because the Pd is insufficient, so the photocatalytic activity of a sample with a Pd content of 0.1 wt.% is slightly lower than that of a sample with a Pd content of 0.5 wt.%. When the Pd content is high, clusters of Pd species form overlapping agglomerates which will shadow the WO_3 by surface plasmon absorption of the Pd nanoparticles [29]. Therefore, there is an optimum Pd content for the dispersion morphology of Pd clusters with high activity. The following experiments were carried out with 0.5 wt.% Pd content.

3.3. Dependence on catalyst loading

To optimize the catalyst loading, a series of experiments were carried out in which the loading was varied from 50 to 250 mg L^{-1} with a dye concentration of 5.0 μmol L^{-1} at 298 K. As a comparison, the direct photolysis of MG was also performed under identical conditions as a control. The degradation efficiency of MG for various catalyst loadings is shown in Fig. 5.

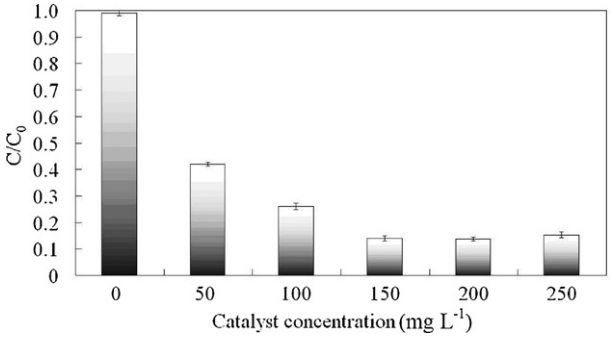

Fig. 5. Dependence on catalyst concentration for the MG degradation after 360 min irradiation over 0.5 wt.% Pd/WO_3. The dye concentration and simulated solar light intensity were the same as those in Fig. 4.

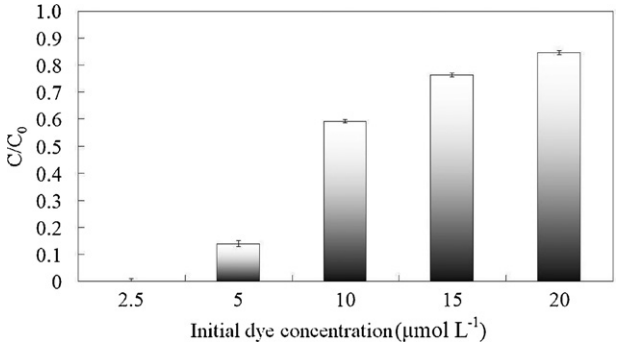

Fig. 6. Dependence on initial dye concentration for the MG degradation after 360 min irradiation over 0.5 wt.% Pd/WO_3. The catalyst concentration and simulated solar light intensity were the same as those in Fig. 4.

As shown in Fig. 5, the MG concentration in the control exhibited no obvious change after being irradiated for 360 min, which indicates that it is almost impossible to photolyze MG under such solar light irradiation. The results also indicate that the photocatalytic efficiency increases up to a maxima as a function of catalyst loading, and tends to decrease upon further loading which is in agreement with a number of studies reported earlier [1,2,30]. The increase in the catalyst loading from 50 to 150 mg L^{-1} sharply increases the dye degradation. The increasing catalyst loading induces an increase in the availability of active sites on the catalyst surface at which MG can be adsorbed. Moreover, the increased amount of catalyst produces a proportional increase in the number of active radicals by absorbing increased numbers of photons, which are sufficient and readily accessible for the degradation of nearby MG. The degradation efficiency remains almost constant with an increase in the catalyst loading from 150 to 200 mg L^{-1}, which suggests that there is an optimal level for catalyst effectiveness. However, loading above 200 mg L^{-1} does not increase the degradation efficiency any further. This phenomenon may be due to the aggregation of a high concentration of catalyst, which could reduce the total active surface area available for adsorbing MG and absorbing light radiation. On the other hand, a higher concentration of catalyst creates turbidity, which is capable of reducing the penetration intensity of light radiation by the scattering effect [31]. So the optimal amount of catalyst was 150–200 mg L^{-1} with an MG concentration of 5.0 μmol L^{-1}. Since the maximum MG degradation was observed with 150 mg L^{-1} of Pd/WO_3 catalyst, the other experiments were performed at this concentration.

3.4. Effect of MG concentration

The photocatalytic degradation at different initial concentrations of MG in the range 2.5–20 μmol L^{-1} was studied. As shown in Fig. 6, the photocatalytic degradation efficiency of MG by Pd/WO_3 under the simulated solar light was found to decrease with increase in concentration of MG. As MG concentration increases, more MG molecules will be adsorbed on the surface of Pd/WO_3, whereas O_2 molecules, the electron acceptor in photocatalysis, will be less [32,33]. In addition, more MG will absorb much light required in the photocatalysis [33]. Consequently, the photodegradation efficiency became lower.

3.5. Spectral changes of MG during degradation

Fig. 7 shows the changes in the MG absorption spectra during photocatalytic degradation with Pd/WO_3 at different irradiation times varying from 0 to 360 min. More than 50% of the MG is degraded within 180 min of irradiation. The results show that the absorption of the visible band at 618 nm decreased and a hypsochromic shift occurred simultaneously with increasing illumination time. The hypsochromic shift may be caused by an N-demethylation process [4,34]. The absorbance peaks at 425 and 315 nm have obviously declined, which indicates that the entire conjugated chromophore structure of MG has been destroyed [4].

3.6. Kinetic analysis

The photocatalytic oxidation kinetics of many dye compounds have often been modeled with the Langmuir-Hinshelwood equation expressed as Eq. (1):

$$r = \frac{dC}{dt} = \frac{kKC}{(1+KC)} \quad (1)$$

since KC is very small compared with 1, by neglecting KC in the denominator and integrating with respect to time t, Eq. (1) can be simplified to a pseudo first order kinetic equation (Eq. (2)):

$$\ln\left(\frac{C_0}{C}\right) = kKt = k_{app}t \quad (2)$$

where r is the reaction rate (μmol L^{-1} min^{-1}), C_0 is the initial concentration of the dye (μmol L^{-1}); C is the concentration of the dye at time t (μmol L^{-1}), t is the irradiation time (min), k is the reaction rate constant (min^{-1}), K is the adsorption coefficient of dye on a photocatalyst particle (L μmol^{-1}).

The kinetic curves for the degradation of MG shown in Fig. 8 follow pseudo first order kinetics as confirmed by the linear transform $\ln(C_0/C) = k_{app}t$. The apparent reaction rate constants (k_{app}) for the photocatalytic degradation of MG were evaluated from experimental data (Fig. 8) using a linear regression. In all cases, the R^2 (correlation coefficient) values are higher than 0.99, which confirms the proposed kinetics for MG decolorization in this process. As expected, increasing the light intensity greatly increases the rate

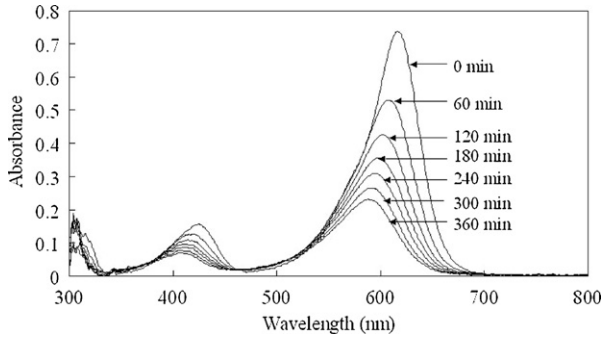

Fig. 7. Absorption spectra of MG at different irradiation times over 0.5 wt.% Pd/WO_3. The experimental conditions were the same as those in Fig. 4.

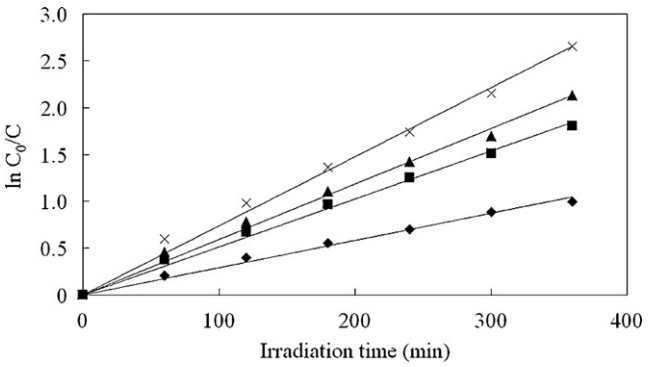

Fig. 8. Analysis of the MG degradation data at (♦) 0.2 mW cm^{-2}, (■) 0.4 mW cm^{-2}, (▲) 0.6 mW cm^{-2} and (×) 0.8 mW cm^{-2} light intensities over 0.5 wt.% Pd/WO_3. The experimental conditions were the same as those in Fig. 4.

of MG degradation. At higher radiation intensity, more reactive species are generated in solution, which in turn are available to react with and degrade the MG molecules.

3.7. Reaction mechanism

When photons with energy ($h\upsilon$) equal to or greater than the semiconductor bandgap are absorbed by WO_3, electron–hole pairs (e_{cb}^-/h_{vb}^+) are generated in WO_3 (Eq. (3)).

$$Pd/WO_3 \rightarrow e_{cb}^- + h_{vb}^+ \quad (3)$$

Then, the photogenerated electron–hole pairs will migrate to the surface of the catalyst and react with the species adsorbed on the surface (e.g. Eqs. (4) and (5)). These reactions prevent the electron–hole pairs from combining.

$$O_2 + 2e_{cb}^- + 2H^+ \rightarrow H_2O_2 \quad (4)$$

$$H_2O + h_{vb}^+ \rightarrow {}^\bullet OH + H^+ \quad (5)$$

However, if the photogenerated electron–hole pairs are not consumed by the locally absorbed species, they must be recombined, which reduces the efficiency of the reaction. The degradation rate of MG with Pd/WO_3 was much higher than that with pure WO_3 which indicates that Pd improves the multiple electron transference to oxygen.

On the other hand, when a colored organic compound is present, a sensitized photocatalytic process may also be able to operate, in which case the adsorbed dye molecules are excited by visible light and thus act as photo-sensitizers. The absorption edge of WO_3 is at approximately 460 nm as shown in Fig. 1, and this is consistent with previously reported values [20,35,36]. As a result the photocatalytic degradation experiments were conducted under visible light ($\lambda > 470$ nm) to investigate the dye sensitization effect by using a cutoff filter (Y-47, Asahi Techno Glass Co. Ltd., Japan) to exclude light with a wavelength of less than 470 nm. Fig. 9 shows the photocatalytic degradation of MG with WO_3 and Pd/WO_3 under visible light ($\lambda > 470$ nm) and with Pd/WO_3 under solar light as a comparison. WO_3 catalyst cannot be excited under visible light ($\lambda > 470$ nm) irradiation, therefore changes in the concentration can be related to sensitization assisted photocatalytic reactions.

The result in Fig. 9 shows that when visible light ($\lambda > 470$ nm) is used, MG degradation takes place with both WO_3 and Pd/WO_3, but a much higher degradation rate was obtained by using Pd/WO_3 than with WO_3 only. This indicates the existence of photosensitized electron injection, leading to dye degradation with light whose energy is lower than the band energy of the photocatalysts. According to this scheme, the photooxidation of the dye is converted to a cationic

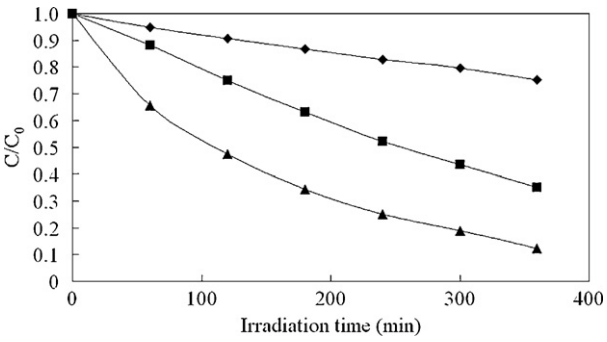

Fig. 9. Comparison of MG degradation with (♦) WO_3 and (■) Pd/WO_3 under visible light ($\lambda > 470$ nm) and with (▲) Pd/WO_3 under simulated solar light irradiation. The experimental conditions were the same as those in Fig. 4.

dye radical by losing an electron in the excited state (Eq. (6)).

$$MG_{ads}* + Pd/WO_3 \rightarrow MG_{ads}{}^{\bullet+} + Pd/WO_3(e^-) \quad (6)$$

$$O_2 + 2e_{cb}^- + 2H^+ \rightarrow H_2O_2 \quad (7)$$

$$H_2O_2 \rightarrow 2{}^\bullet OH \quad (8)$$

$${}^\bullet OH(or H_2O_2) + MG \rightarrow \text{products} \quad (9)$$

$$MG_{ads}{}^{\bullet+} \rightarrow \text{products} \quad (10)$$

The injected electron can be then scavenged by adsorbed oxygen to produce H_2O_2 (Eq. (7)), and the H_2O_2 may subsequently generate hydroxyl radicals (•OH) (Eq. (8)). The active radicals produced in the above manner can then react with the dye to form other species and are thus responsible for the discoloration of the MG (Eq. (9)). The self-sensitized mechanism and the effect of Pd are shown in Fig. 10.

In the case of irradiation with simulated solar light (Fig. 11), Pd improves the MG degradation efficiency. Here, Pd acts as a trap

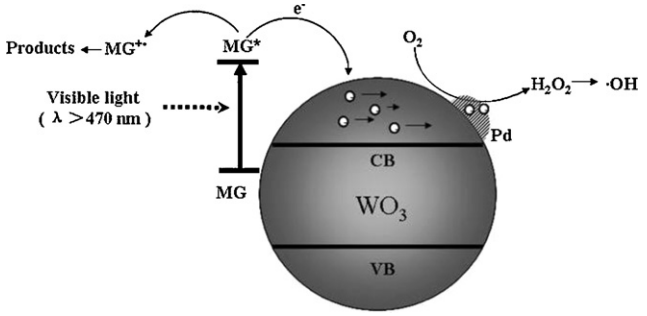

Fig. 10. Mechanism of the MG degradation using Pd/WO_3 under visible light ($\lambda > 470$ nm) irradiation.

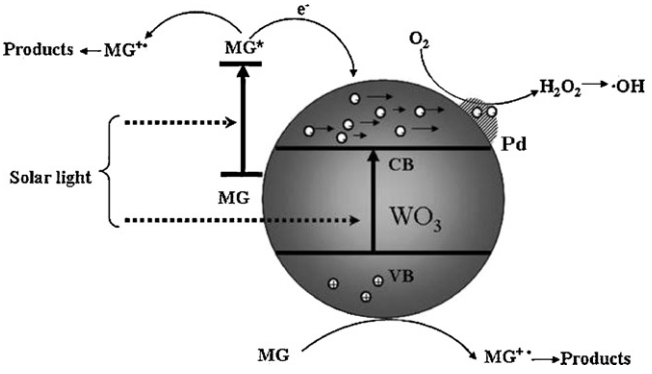

Fig. 11. Mechanism of the MG degradation using Pd/WO_3 under simulated solar light irradiation.

for both the photoexcited electrons of WO_3 and the self-sensitized electrons of MG. The dye sensitization and the Pd modification used for the multiple electron transference to oxygen may have some synergetic effect in the present stage.

4. Conclusion

The photocatalytic degradation of MG was investigated by using a Pd/WO_3 photocatalyst under simulated solar light illumination. A 0.5 wt.% Pd/WO_3 sample exhibited the best photocatalytic activity and the optimum catalyst loading was 150 mg L^{-1}. Pd nanoparticles effectively enhanced the photocatalytic activity of WO_3 as well as the self-sensitized degradation of MG by suppressing the recombination of electron–hole pairs. The data were successfully analyzed with the Langmuir-Hinshelwood pseudo first order kinetic model under different light intensities. The degradation rate increased with increasing light intensity. The electrons are considered to accumulate on Pd, which promotes the reduction of oxygen molecules. To the best of our knowledge, this is the first evidence that Pd on WO_3 promotes electron transfer to oxygen molecules even though the electrons originated from MG via the self-sensitization mechanism. The present results indicate that using Pd/WO_3 may be a good strategy for the efficient purification of wastewater or the algal originated dirt on walls under solar irradiation.

Acknowledgements

This work was partly supported by government initiated R&D projects for small and medium sized enterprises (SMEs) in standards development FY 2007. We are grateful to Yutaka Hyodo and Kunio Uchida for their technical assistance with the TEM and the Autosorb-1 analyzer.

References

[1] M. Farooq, I.A. Raja, A. Pervez, Photocatalytic degradation of TCE in water using TiO_2 catalyst, Sol. Energy 83 (2009) 1527–1533.
[2] A.A. Ismail, Single-step synthesis of a highly active photocatalyst for oxidation of trichloroethylene, Appl. Catal. B: Environ. 85 (2008) 33–39.
[3] M.M. Joshi, N.K. Labhsetwar, P.A. Mangrulkar, S.N. Tijare, S.P. Kamble, S.S. Rayalu, Visible light induced photoreduction of methyl orange by N-doped mesoporous titania, Appl. Catal. A: Gen. 357 (2009) 26–33.
[4] Y.M. Ju, S.G. Yang, Y.C. Ding, C. Sun, A.Q. Zhang, L.H. Wang, Visible light induced photoreduction of methyl orange by N-doped mesoporous titania, J. Phys. Chem. A 112 (2008) 11172–11177.
[5] S.K. Mohapatra, N. Kondamudi, S. Banerjee, M. Misra, Functionalization of self-organized TiO_2 nanotubes with Pd nanoparticles for photocatalytic decomposition of dyes under solar light illumination, Langmuir 24 (2008) 11276–11281.
[6] S.K. Pardeshi, A.B. Patil, A simple route for photocatalytic degradation of phenol in aqueous zinc oxide suspension using solar energy, Sol. Energy 82 (2008) 700–705.
[7] H. Tian, J.F. Ma, K. Li, J.J. Li, Photocatalytic degradation of methyl orange with W-doped TiO_2 synthesized by a hydrothermal method, Mater. Chem. Phys. 112 (2008) 47–51.
[8] A. Watcharenwong, W. Chanmanee, N.R. de Tacconi, C.R. Chenthamarakshan, P. Kajitvichyanukul, K. Rajeshwar, Anodic growth of nanoporous WO_3 films: morphology, photoelectrochemical response and photocatalytic activity for methylene blue and hexavalent chrome conversion, J. Electroanal. Chem. 612 (2008) 112–120.
[9] Z.G. Zhao, M. Miyauchi, Nanoporous-walled tungsten oxide nanotubes as highly active visible-light-driven photocatalysts, Angew. Chem. Int. Ed. 47 (2008) 7051–7055.
[10] M. Sathish, B. Viswanathan, R.P. Viswanath, C.S. Gopinath, Synthesis, characterization, electronic structure, and photocatalytic activity of nitrogen-doped TiO_2 nanocatalyst, Chem. Mater. 17 (2005) 6349–6353.
[11] J.J. Xu, Y.H. Ao, D.G. Fu, A novel Ce, C-codoped TiO_2 nanoparticles and its photocatalytic activity under visible light, Appl. Surf. Sci. 256 (2009) 884–888.
[12] Z.B. Wu, F. Dong, Y. Liu, H.Q. Wang, Enhancement of the visible light photocatalytic performance of C-doped TiO_2 by loading with V_2O_5, Catal. Commun. 11 (2009) 82–86.
[13] C.F. Lin, C.H. Wu, Z.N. Onn, Degradation of 4-chlorophenol in TiO_2, WO_3, SnO_2, TiO_2/WO_3 and TiO_2/SnO_2 systems, J. Hazard. Mater. 154 (2008) 1033–1039.
[14] M. Miyauchi, M. Shibuya, Z.G. Zhao, Z.F. Liu, Photocatalysis and photoinduced hydrophilicity of WO_3 thin films with underlying Pt nanoparticles, J. Phys. Chem. C 113 (2009) 10642–10646.
[15] T. Torimoto, N. Nakamura, S. Ikeda, B. Ohtani, Discrimination of the active crystalline phases in anatase–rutile mixed titanium(IV) oxide photocatalysts through action spectrum analyses, Phys. Chem. Chem. Phys. 4 (2002) 5910–5914.
[16] M. Miyauchi, Photocatalysis and photoinduced hydrophilicity of WO_3 thin films with underlying Pt nanoparticles, Phys. Chem. Chem. Phys. 10 (2008) 6258–6265.
[17] T. Arai, M. Horiguchi, M. Yanagida, T. Gunji, H. Sugihara, K. Sayama, Complete oxidation of acetaldehyde and toluene over a Pd/WO_3 photocatalyst under fluorescent- or visible-light irradiation, Chem. Commun. 43 (2008) 5565–5567.
[18] T. Arai, M. Horiguchi, M. Yanagida, T. Gunji, H. Sugihara, K. Sayama, Reaction mechanism and activity of WO_3-catalyzed photodegradation of organic substances promoted by a CuO cocatalyst, J. Phys. Chem. C 113 (2009) 6602–6609.
[19] T. Arai, M. Yanagida, Y. Konishi, A. Ikura, Y. Iwasaki, H. Sugihara, K. Sayama, The enhancement of WO_3-catalyzed photodegradation of organic substances utilizing the redox cycle of copper ions, Appl. Catal. B: Environ. 84 (2008) 42–47.
[20] Y.H. Kim, H. Irie, K. Hashimoto, A visible light-sensitive tungsten carbide/tungsten trioxde composite photocatalyst, Appl. Phys. Lett. 92 (2008).
[21] M. Maalej-Kammoun, H. Zouari-Mechichi, L. Belbahri, S. Woodward, T. Mechichi, Malachite green decolourization and detoxification by the laccase from a newly isolated strain of *Trametes* sp., Int. Biodeterior. Biodegrad. 63 (2009) 600–606.
[22] S. Rehman, R. Ullah, A.M. Butt, N.D. Gohar, Strategies of making TiO_2 and ZnO visible light active, J. Hazard. Mater. 170 (2009) 560–569.
[23] G.R. Bamwenda, H. Arakawa, The visible light induced photocatalytic activity of tungsten trioxide powders, Appl. Catal. A: Gen. 210 (2001) 181–191.
[24] N. Le Houx, G. Pourroy, F. Camerel, M. Comet, D. Spitzer, WO_3 Nanoparticles in the 5–30 nm range by solvothermal synthesis under microwave or resistive heating, J. Phys. Chem. C 114 (2010) 155–161.
[25] S. Fardindoost, A.I. Zad, F. Rahimi, R. Ghasempour, Pd doped WO_3 films prepared by sol–gel process for hydrogen sensing, Int. J. Hydrogen Energy 35 (2010) 854–860.
[26] L. Ge, Novel $Pd/BiVO_4$ composite photocatalysts for efficient degradation of methyl orange under visible light irradiation, Mater. Chem. Phys. 107 (2008) 465–470.
[27] L.X. Wang, S.L. Xu, W.L. Chu, W.S. Yang, Effect of Pd loading and precursor on the catalytic performance of Pd/WO_3–ZrO_2 catalysts for selective oxidation of ethylene, Catal. Today 149 (2010) 163–166.
[28] Y.L. Liu, L.J. Guo, W. Yan, H.T. Liu, A composite visible-light photocatalyst for hydrogen production, J. Power Sources 159 (2006) 1300–1304.
[29] M. Shibuya, M. Miyauchi, Site-selective deposition of metal nanoparticles on aligned WO_3 nanotrees for super-hydrophilic thin films, Adv. Mater. 21 (2009) 1373–1376.
[30] M. Qamar, M.A. Gondal, K. Hayat, Z.H. Yamani, K. Al-Hooshani, Laser-induced removal of a dye CI Acid Red 87 using n-type WO_3 semiconductor catalyst, J. Hazard. Mater. 170 (2009) 584–589.
[31] B. Neppolian, H.C. Choi, S. Sakthivel, B. Arabindoo, V. Murugesan, Solar light induced and TiO_2 assisted degradation of textile dye reactive blue 4, Chemosphere 46 (2002) 1173–1181.
[32] C.S. Lu, Y.T. Wu, F.D. Mai, W.S. Chung, C.W. Wu, W.Y. Lin, C.C. Chen, Degradation efficiencies and mechanisms of the ZnO-mediated photocatalytic degradation of Basic Blue 11 under visible light irradiation, J. Mol. Catal. A: Chem. 310 (2009) 159–165.
[33] M.A. Rauf, S.S. Ashraf, Fundamental principles and application of heterogeneous photocatalytic degradation of dyes in solution, Chem. Eng. J. 151 (2009) 10–18.
[34] M.A. Behnajady, N. Modirshahla, M. Shokri, B. Vahid, Effect of operational parameters on degradation of Malachite Green by ultrasonic irradiation, Ultrason. Sonochem. 15 (2008) 1009–1014.
[35] M. Miyauchi, A. Nakajima, T. Watanabe, K. Hashimoto, Photocatalysis and photoinduced hydrophilicity of various metal oxide thin films, Chem. Mater. 14 (2002) 2812–2816.
[36] M. Miyauchi, A.K. Nakajima, T. Watanabe, K. Hashimoto, Photoinduced hydrophilic conversion of TiO_2/WO_3 layered thin films, Chem. Mater. 14 (2002) 4714–4720.